Negative capacitance as a diagnostic tool for recombination in purple quantum dot LEDs

View Online Export Citation CrossMark

Christian Blauth,[1,2] (iD) Paul Mulvaney,[1] (iD) and Tadahiko Hirai[2,a)] (iD)

AFFILIATIONS

[1]ARC Centre of Excellence in Exciton Science, School of Chemistry, University of Melbourne, Parkville, Victoria 3010, Australia
[2]CSIRO Manufacturing, Bayview Avenue, Clayton, Victoria 3168, Australia

[a)]Electronic mail: tadahiko.hirai@csiro.au

ABSTRACT

Impedance spectroscopy is a powerful and nondestructive tool for studying charge carrier dynamics in quantum dot light-emitting diodes (QLEDs). We report here that QLEDs exhibit unique capacitance behavior that strongly depends on the ligand chemistry of the quantum dots (QDs). At low frequencies and under bipolar injection, the capacitance of the QLEDs becomes negative before it returns to positive values at even lower frequencies. This behavior is fundamentally different from that observed in organic light-emitting diodes and is attributed to the accumulation of charge carriers within the ligand shells during operation. The capacitive response depends on both the conductivity and the length of the QD ligands and can be used as a diagnostic tool for understanding the luminescent recombination efficiency of a QLED. We find that short and conductive ligands result in positive device capacitances only and this correlates with enhanced device efficiency.

Published under license by AIP Publishing. https://doi.org/10.1063/1.5088177

I. INTRODUCTION

Over the last few decades, tremendous improvements in lifetime and brightness have enabled the integration of red and green as well as white organic light emitting diodes (OLEDs) into smartphone displays and TV screens.[1–6] With a 50% brightness drop after 200 000 h of operation at 1000 cd/m^2, and an efficiency of over 30 cd/A for red and 70 cd/A for green emitting devices, these solution processed OLEDs exhibit astounding long term stability. Conversely, blue/purple OLEDs exhibit lifetimes of several thousand hours only and typically display decreased efficiencies of around 10 cd/A.[2,7] Furthermore, their emission is spectrally broad, typically reaching into the green and red.[2]

Light-emitting semiconductor quantum dots (QDs) have recently garnered attention because of their potential application in next generation, high-performance displays and solid-state lighting.[8–10] QDs in principle show greater photostability than organic flourophores and possess size-tunable narrow-band emission spectra reaching from the UV to NIR spectral regions.[8,11–13] Since the first report of a quantum dot light emitting diode (QLED) in 1994,[14] their performance has increased due to improved synthetic routes, as well as development of more sophisticated device architectures,[10] with recent devices displaying brightnesses of over

50 000 cd/m^2 for green light, over 45 000 cd/m^2 for red light, and over 10 000 cd/m^2 for blue wavelengths.[15] The reduced performance of blue QLEDs mainly originates from the larger optical bandgap, the presence of more trap states, higher loss factors, and the increased difficulties in efficiently injecting charge carriers into the QDs. For blue emission at 452 nm, high operating voltages of over 5 V are required to reach a brightness of over 100 cd/m^2, which decreases the luminous power efficiency and the overall lifetime of the device.[10,16] These problems are further exacerbated for shorter emissive wavelengths, making purple QLEDs more challenging to fabricate.

Impedance spectroscopy (IS) is a powerful and nondestructive tool for the characterization of optoelectronic devices; it is particularly suited to study the effect of trap states in large bandgap QD devices and their impact on recombination and device performance as a whole. IS has been widely used in OLEDs to determine the injection of charge carriers,[17,18] their transport and mobility through localized states,[19,20] and finally to determine degradation of electrically aged OLEDs.[21] Changes in capacitance reflect the changes in density of charge carriers within the active layer and can be used to capture complex and unusual electrical responses, with the phenomenon of

negative capacitance (NC) being perhaps the most prominent example.[22] The NC effect has been reported in various electronic devices, such as crystalline and amorphous semiconductors, as well as in organic and nanoparticle devices spanning GaAs IR detectors, superconductors, and OLEDs.[23–32] As fundamentally different as these devices are, so are the origins of NC, ranging from contact problems which cause parasitic resistances in series,[22,33] to interface[24] and minority injection[34] problems.

Many systems exhibiting NC consist of a conductor or a semiconductor sandwiched between two electrical contacts, with charge carriers stored and released from trap states when a sufficient bias and ac-voltage are applied. This phenomenon is enhanced in thin interface layers[31,35] and is theoretically described by a positive-valued time derivative of the transient current response to a voltage step.[22]

IS has been applied to QDs integrated into solar cells, with their superior performance electrically modeled through equivalent circuits.[36,37] The recombination pathways of QD sensitized[37] and core/shell QD solar cells[38] have also been reported. Uddin and Teo[39] have studied the differential capacitance of a hybrid QD/organic LED, where the total capacitance of the device can drop below 0 based on the formation of a time-dependent transient current originating from the organic/QD interfacial states. However, this study does not consider the role of recombination pathways in the formation of NC.

In this report, IS is used to study the capacitive and recombinative behavior of charge carriers in purple QLEDs emitting at 410 nm (Fig. 6). We show that varying the length and conductivity of the capping ligand determines the accumulation of injected charge carriers in the active QD layer. A simple numerical model qualitatively describes the impact of electron and hole accumulation on capacitance. Luminescent recombination leads to a slight drop in capacitance, whereas nonluminescent recombination and the formation of a recombination current are both ligand dependent and lead to negative device capacitances. The dependence of the capacitance on frequency can be used as an indicator for device performance.

II. EXPERIMENTAL PROCEDURES

The QDs were synthesized following a protocol developed by Bae et al.,[40] whereby 0.5 mmol of cadmium oxide (CdO) (99.95%), 5 mmol of zinc acetate dihydrate [Zn(acet)$_2$] (>98%, reagent grade), 7 ml of 1-octadecene (ODE) (tech grade, 90%), and 3.5 ml of oleic acid (OA) (tech grade, 90%) were first placed in a 50 ml round bottom flask. The mixture was heated to 100 °C and degassed under vacuum for 1 h before it was heated to 310 °C under N_2 to form a transparent solution of the metal oleates, Cd(OA)$_2$ and Zn(OA)$_2$. At this temperature, 3 mmol of sulfur powder (99.98%) dissolved in 3 ml of 1-ODE, which was heated to 150 °C, was swiftly injected into the reaction flask to trigger the growth of Cd$_{1-x}$Zn$_x$S cores. After 6 min, 4 mmol of sulfur powder dissolved in tributylphosphine (TBP) (97%) was introduced into the reactor to overcoat the existing Cd$_{1-x}$Zn$_x$S cores with a ZnS shell. The reaction was stopped after 70 min, and the flask cooled down to room temperature. The QDs were purified through 3 centrifuge steps: the crude solution was washed by adding acetone until the solution became turbid, usually

by doubling the volume. The addition of small amounts of ethanol helped to quantitatively precipitate the particles. The precipitate was collected after centrifugation at 4000 rpm and redispersed in a minimal volume of toluene. The batch was then split into 5 parts and a ligand exchange was performed: For the insulating ligands [butylamine (99%), octylamine (99%), and oleylamine (70%, technical grade)], an excess of the appropriate amine was added to the QD solution while for the electrically conducting ligands [aniline (>99.5%) and triphenylamine (98%)] a 1–10 wt. % was added based on the ligand to QD mass ratio and determined by UV-VIS absorption spectroscopy. All QDs were precipitated another 3 times to ensure that nonbinding ligands were washed away. UV-VIS absorption and fluorescence spectra of the ligand exchanged quantum dots are shown in Fig. 5.

The QLEDs in this study were prepared in a clean room environment and designed in a sandwich architecture based on a patterned 150 nm thick indium tin oxide (ITO) covered glass substrate. The substrates were cleaned in an ultrasonicator with ethanol and water. A 70 nm thick PEDOT:PSS (Al 4083) layer was deposited by spin coating. After annealing at 200 °C for 10 min a 50 nm thick poly(9-vinylcarbazole) (PVK) film was cast from a 10 mg/ml chlorobenzene solution and annealed for 30 min at 180 °C. The samples were then transferred into a nitrogen filled glove box. A 25 nm QD film was deposited from toluene by spin coating and dried at 120 °C for 20 min. A 25 nm thick layer of 3,3′,5,5′-tetra[(m-pyridyl)-phen-3-yl]biphenyl (BP4mPy) was thermally deposited as the electron transport layer followed by a LiF/Al (1 nm/100 nm) electrode.

All chemicals were purchased from Sigma Aldrich and were used without further purification. Acetone and ethanol were purchased as analytical grade from Univar, toluene and chlorobenzene from ChemSupply TBP from Capot Chemical Co. Ltd., PEDOT:PSS was purchased from Heraus Clevios, PVK [>99% (HPLC)] and BP4mPy [>99% (HPLC)] from Luminescence Technology Corp. UV-visible absorbance measurements were performed on an HP Agilent 8453 spectrophotometer. Fluorescence emission and excitation spectra were recorded on a Horiba Jobin Yvon Fluorolog-3 spectrometer. Luminescence and $I–V$ characteristics were obtained with a luminescence color meter (Topcon MB-7A) and a Keithley 2400 source-measure unit. A Solartron SI-1255 and a frequency response analyser system were used for the IS and capacitance measurements.

III. SIMPLE NUMERICAL MODEL

Negative capacitance NC has the same small-signal voltage and current relationship as positive inductance $L = j\omega L = -\frac{1}{j\omega C}$.[22] However, the treatment of NC as an inductance is not meaningful, because a QLED does not produce a significant magnetic field nor does it display an inductance that increases with frequency. A more suitable interpretation of a NC is based on an analysis of the transient current $\delta j(t)$ response to a voltage step. The total capacitance can then be described through Eq. (1), as the sum of $C_0 = C(\infty)$ as the geometric, frequency independent capacitance and a frequency trap state dependent capacitance. A decrease in capacitance occurs if the function $-d\delta j(t)/dt$ is negative and monotonically increasing to 0, making $C(\omega)$ negative.[22,27] In the case of a small negative value of $-d\delta j(t)/dt$, the total capacitance can decrease but remain positive, which we refer to here as decreasing capacitance. If the

slope of dj/dt is increased sufficiently, we observe two situations: if capacitance drops below 0 and remains negative, we refer to this as the OLED NC case.[27] Conversely, if C drops below 0, then returns to positive values, we call this the QLED NC case,[39]

$$C(\omega) = C_0 + \frac{1}{\Delta V}\int_0^\infty \delta j(t)\cos(\omega t)dt. \qquad (1)$$

The physical origin of the transient current response to a voltage step, and its effect on the frequency-dependent capacitance, can be broad. In this study, we propose that the ligand-dependent accumulation of charge carriers as additional cause contributing to the formation of NC. For an optoelectronic device, we assume that capacitance depends on the accumulation and recombination of charge carriers. When electrons and holes are injected into the active layer and recombine at a finite rate, a finite volume exists where electrons and holes overlap, leading to a recombination current.[27] Therefore, let us consider the transient current response of positive and negative exponential components, using Eq. (2),[22]

$$\Delta j(t) = \Delta V\{a_1\exp(-t/\tau_1) - (a_2\exp(-t/\tau_2)\}, \qquad (2)$$

where a_1 is an arbitrary constant and τ_1 are the accumulation constant and the related time constant, respectively, whereas a_2 and τ_2 are the equivalent recombination constants. The capacitance corresponding to this transient is shown in Eq. (3),

$$\begin{aligned} C(\omega) &= C_0 + C_{acu} - C_{rec} \\ &= C_0 + \frac{a_1\tau_1}{1+(\omega\tau_1)^2} - \frac{a_2\tau_2}{1+(\omega\tau_2)^2}. \end{aligned} \qquad (3)$$

A. Relation to numerical model

Assuming that a ligand variation mainly affects the accumulation and transport of charge carriers and has only a small effect on their recombination properties, the impact of the accumulation parameter a_1 can be modeled. The details of the numerical model are listed in Table I. An accumulation of charge carriers leads to an increase in the capacitance as more charge carriers are stored.[41,42] During recombination, electrons and holes recombine and the population of charge carriers is reduced; hence, the capacitance decreases.[43]

Figure 1 summarizes the impact of a_1 on the behavior of the capacitance, both in a linear and in a logarithmic plot.[39] In the OLED NC [Fig. 1(c)], the capacitance drops below 0 at a defined threshold frequency and stays negative for decreasing frequencies.[27,39,44,45] Under fixed recombination conditions, the accumulation is lowest in this case and we, therefore, assume that luminescent recombination is dominant. If the accumulation constant is increased, the decreasing C [Fig. 1(a)] is achieved. In this case, the

TABLE I. Overview of the simulation parameters for the three different cases of negative capacitance in QLEDs.

	C_0	a_1	τ_1	a_2	τ_2
OLED NC	10^{-9}	10^{-6}	2	$2\cdot10^{-5}$	1.4
Decreasing C	10^{-9}	$1.5\cdot10^{-5}$	2	$2\cdot10^{-5}$	1.4
QLED NC	10^{-9}	$2.84\cdot10^{-5}$	2	$2\cdot10^{-5}$	1.4

total capacitance remains positive for all frequencies and only decreases slightly for low frequencies before it increases for even lower frequencies. In this case, the accumulation is strong enough to maintain a positive capacitance, which is only slightly reduced in case of weak recombination. As the accumulation increases, the capacitance increases and the QD NC case [Fig. 1(e)] is achieved. In this case, the capacitance drops below 0 before it returns to positive values for decreasing frequencies. If more charge carriers are injected, this internal capacitance is discharged by generation of a recombination current. In this case, nonluminescent recombination is dominant. In impedance spectroscopy, this current causes the capacitance to drop below 0.

Experimental data support our model: Fig. 7 shows the luminescence efficiency of a butylamine-capped QLED. At a low bias of 4 V, the efficiency of the device is highest suggesting that most charges recombine under the formation of light and an OLED NC is seen. If the bias is increased, more charges are injected but the device efficiency decreases suggesting that nonluminescent recombination pathways become more dominant and the capacitance follows the QLED NC case.

IV. RESULTS AND DISCUSSION

A. Results of IS measurements

Figure 2 compares the real part of the capacitance $Re(C)$ with imaginary part $Im(Z)$ of the impedance, as well as the capacitance loss factor $\tan(\delta)$ of QLEDs, with different insulating ligands (Appendix A). The areas of negative capacitance are outlined in the C–f plots. Appendix A outlines the principles of an in-phase and out-of-phase component of an electrical capacitance as well as for a quality factor for a capacitance.

At low bias, the capacitance of QLEDs with oleylamine-capped QDs remains almost constant over a frequency range from 0.4 Hz to 200 kHz, as shown in Fig. 2(a). With an increased bias, charge carriers are trapped and, at a bias-dependent threshold frequency the real part of the capacitance increases with decreased frequency. If the applied bias is increased, charge carriers are trapped at higher frequencies and the capacitance increases with the bias. However, in the 10 V case, between 10 Hz and 10 kHz, the capacitance decreases slightly but stays positive, before it reaches its threshold frequency at 40 Hz and increases again. This behaviour is the first indicator of a NC and is referred to here as decreasing capacitance. The QLED with oleylamine-capped ligands shows the highest capacitance in this study. Due to the strong insulating properties of the ligand, injection and transport of charge carriers to the QD and recombination are both reduced and instead a large capacitance is observed [Fig. 2(a)].

As is evident from Fig. 2(b), $Im(Z)$ increases with increasing bias. The threshold frequency for an almost constant $Im(Z)$ moves to higher frequencies with an increased bias, resulting in an increase in the density of charge carriers in the active layer. The value of $\tan\delta$ also increases, which implies the active layer is becoming more electrically conductive, as seen in Fig. 2(c). The dielectric-loss maximum shifts to higher frequencies with an increased bias.

For the QLEDs fabricated with the shorter octylamine ligand, $Re(C)$ increases with an applied bias [Fig. 2(d)]. For a bias of up to 5 V, the capacitive behavior is comparable to the oleylamine

(a) Decreasing C (log)

(b) Decreasing C (lin)

(c) OLED NC (log)

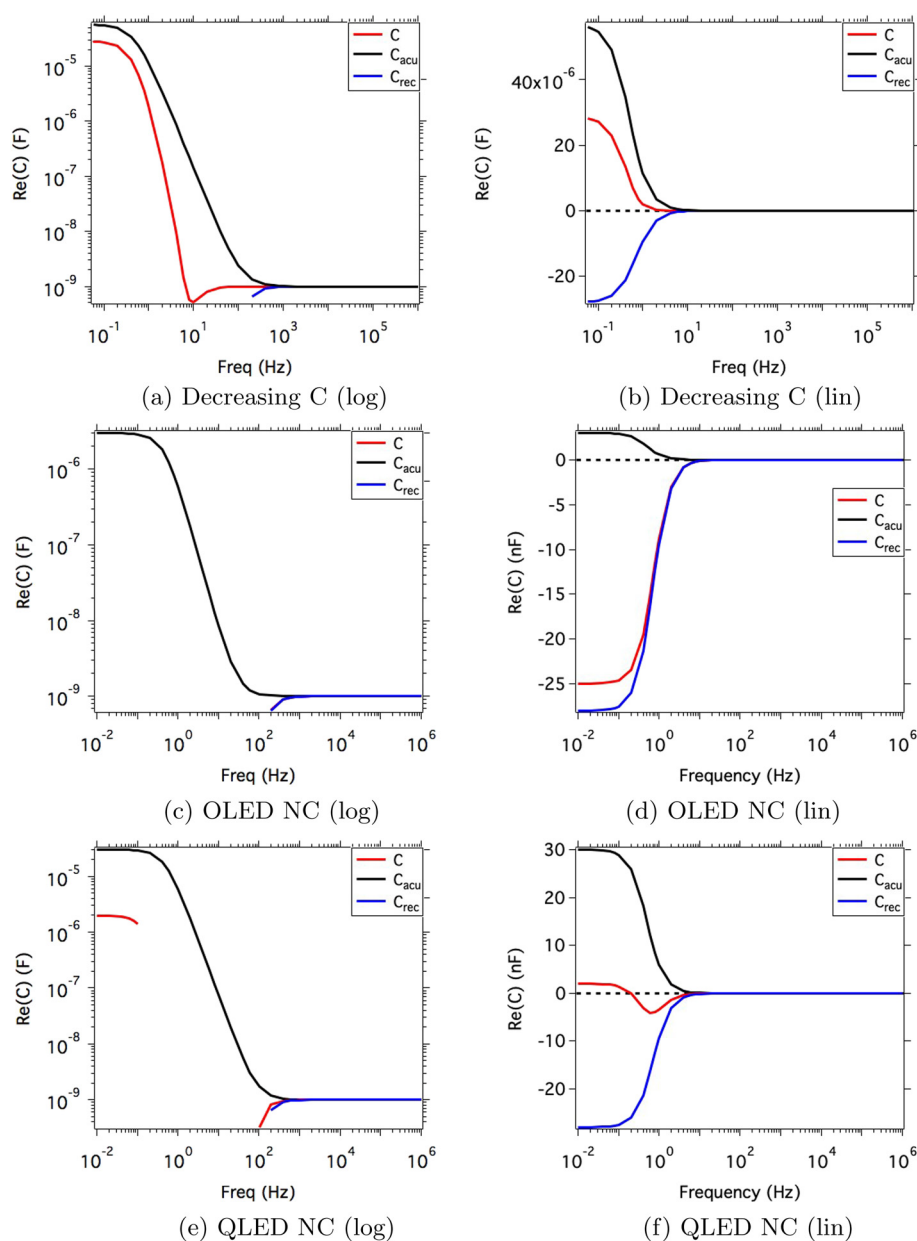(d) OLED NC (lin)

(e) QLED NC (log)

(f) QLED NC (lin)

FIG. 1. Overview of the simulation of the three cases of NC dependent on various accumulation constants. Figures 1(a) and 1(b) (decreasing capacitance), Figs. 1(c) and 1(d) (OLED NC), and Figs. 1(e) and 1(f) (QLED NC) show the different cases of NC in a logarithmic and linear plot, respectively.

analogue with the threshold frequency increasing with the bias. At 6 V, the capacitance decreases but stays positive (decreasing capacitance case). With a further increase in bias, the real part of the capacitance drops below 0 before it reaches positive values for lower frequencies again. This is referred to here as the QLED-NC case. For a negative capacitance, the imaginary part of the impedance becomes positive [Eq. (A4)]. As Fig. 2(f) indicates, the loss factor increase in the NC case is over fivefold and maximizes where $Re(C)$ reaches 0. The loss factor changes sign and then decreases further. Once a critical loss threshold is reached, $Im(Z)$ becomes negative and finally $Re(C)$ becomes positive. With an increased

bias, the threshold frequency for NC shifts to higher frequencies and the frequency range over which NC is observed is enlarged.

As is the case for longer alkylamine cases, $Re(C)$ for butylamine-capped QDs increases with bias from $0 < V < 3$ [Fig. 2(g)], and more charge carriers are injected as $Im(Z)$ increases. With this bias, the losses increase with an increased real part of the capacitance [Fig. 2(i)]. Once the bias is further increased to 5 V, the capacitance drops below 0 and $Im(Z)$ becomes negative. The dielectric losses maximize when the capacitance reaches 0 and again it changes sign to negative as the frequency decreases further [Fig. 2(j)]. The losses decrease further and stay negative throughout the decreasing
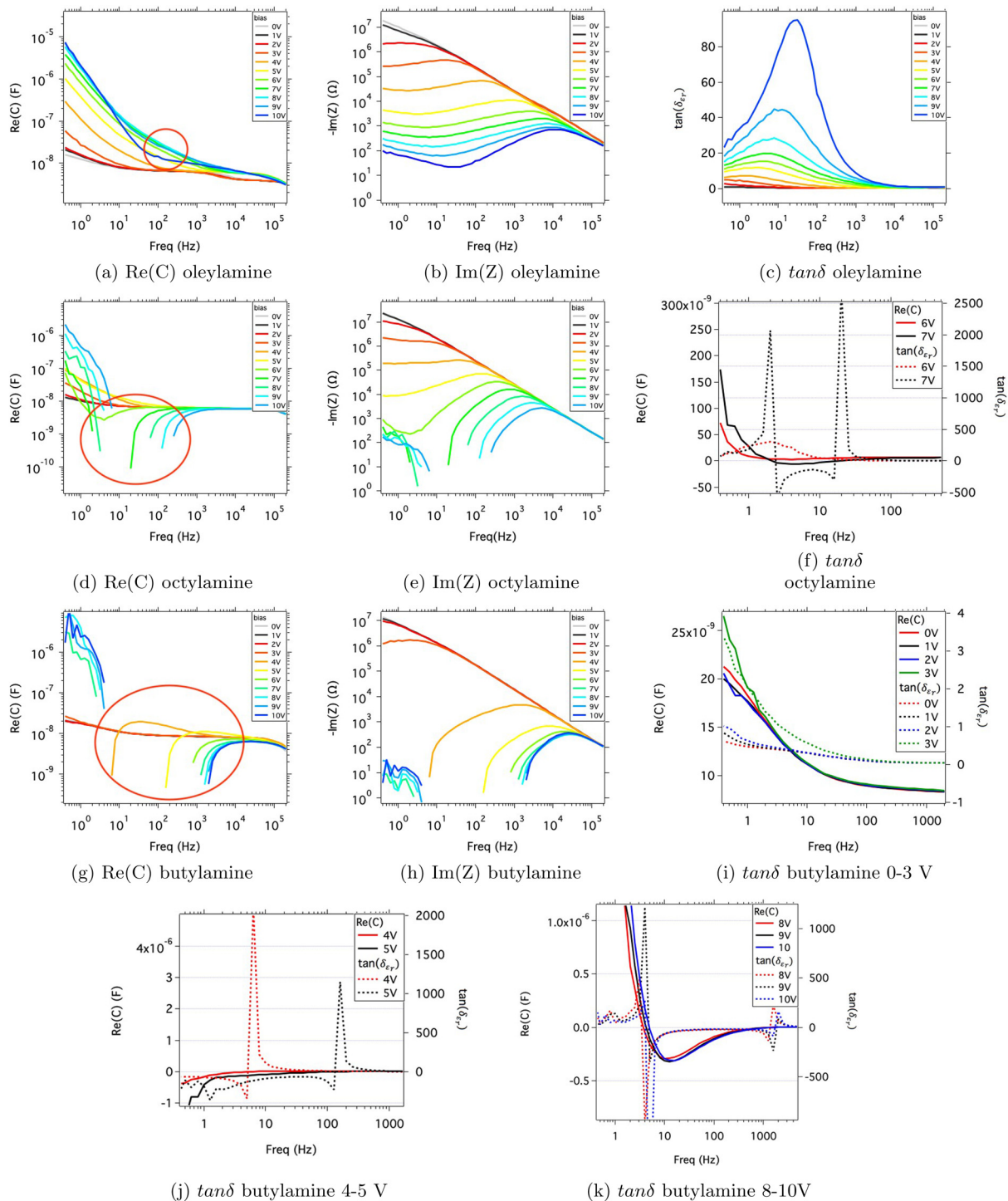
FIG. 2. Summary of the real part of the capacitance, the imaginary part of the impedance, and the capacitance loss factor of a QLED with insulating ligands of different length. Figures 2(a)–2(c) summarise the oleylamine case. Figures 2(d)–2(f) sum up the octylamine case. Figures 2(g)–2(k) conclude the butylamine case.

frequency range. Other than in the octylamine case, the capacitance does not return to positive values. This case is very similar to the typical OLED NC case, as reported by Ehrenfreund et al.[27] If the bias is further increased, the "QLED NC" case is established, with the capacitance value dropping below 0 and returning to positive values as the frequency further decreases.

With an increased bias, the dielectric-loss threshold $\tan(\delta)$ for NC decreases [Fig. 2(k)], indicating that NC leads to a reduced capability to store charge carriers within the device and an increase in dielectric loss, as well as a first indicator of degradation. Whereas the luminescence recombination efficiency of a butylamine-capped QLED decreases with bias, the QLED NC case becomes more dominant (Fig. 7).

When the insulating ligands are replaced with conductive ones, as shown in Fig. 3, the capacitance behaviour changes significantly. For the aniline case [Fig. 3(a)], the capacitance increases with bias and the threshold frequency moves to higher frequencies. The capacitance stays positive for all applied biases and only drops slightly. Along with a more pronounced drop in capacitance, the imaginary part of the impedance decreases but does not change sign [Fig. 3(b)]. As in the oleylamine case, the dielectric-loss factor increases with applied bias and its maximum shifts to higher frequencies [Fig. 3(c)]. The similarity between electrically insulating and electrically conducting ligands in regard to their capacitance and impedance response is based on a similar amount of charge

carriers in the active layer. However, the light output differs quite significantly, suggesting that the recombination efficiency differs greatly between the two ligands (Fig. 6).

The triphenylamine is a larger and more conductive ligand than the alkylamines. In QLEDs with triphenylamine-capped QDs, the capacitative response is similar to aniline devices; however, under strong recombination, the QLED NC case is still observed and the capacitance drops below 0 and returns to positive values with decreased frequencies [Fig. 3(d)]. For the NC, the dielectric-loss factor increases almost fivefold compared to the drop NC in the aniline analog [Fig. 3(f)].

B. Discussion

Our explanation for the formation of a negative capacitance is shown in Fig. 4.

In the simplest case, a capacitor consists of two electrodes with a dielectric sandwiched in between. Its capacitance depends on the distance between the plates; the smaller the distance of the plates, the larger the capacitance value. In a QLED, the frequency determines the amount of charge carriers located in the active layer. At a very high frequency, as shown in region A of Fig. 4, the active area is wide, and the capacitance is low. At this frequency, charges get trapped and released at a small time constant making a stationary accumulation of charges difficult. In this case, the
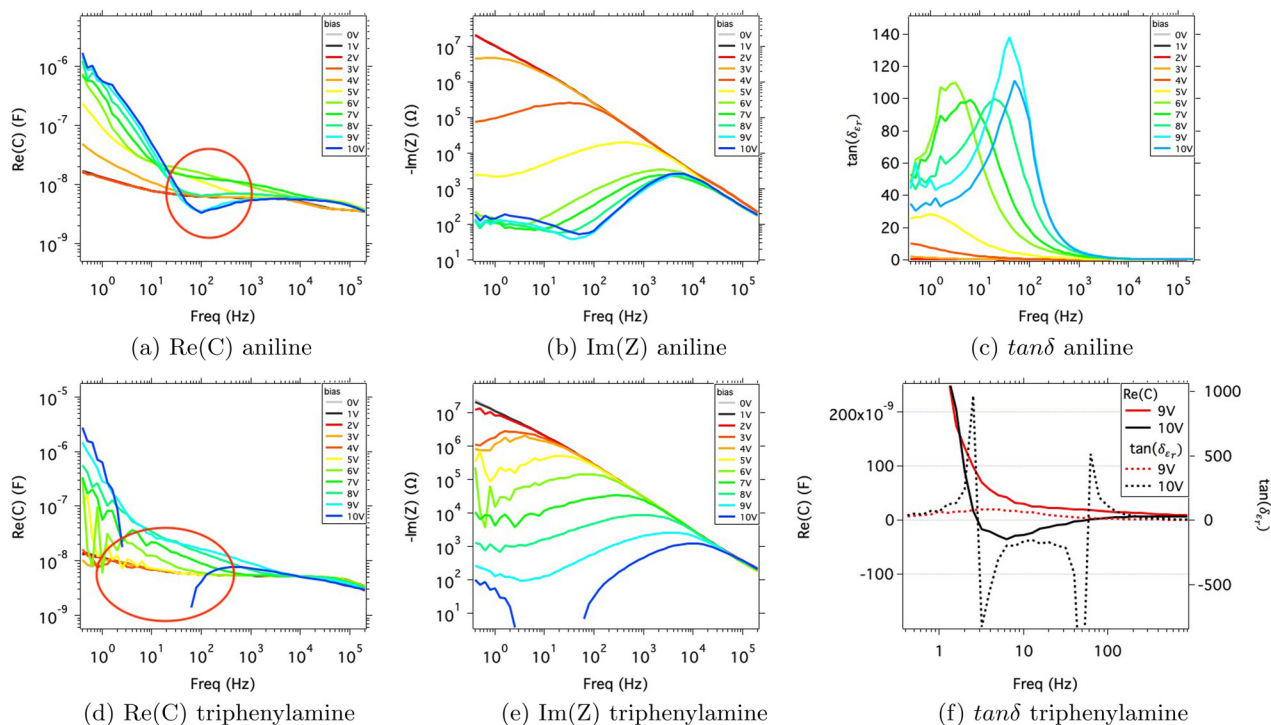

FIG. 3. Summary of the real part of the capacitance, the imaginary part of the impedance, and the capacitance loss factor of a QLED with conductive ligands. Figures 3(a)–3(c) summarize the aniline case. Figures 3(d)–3(f) sum up the triphenylamine case.
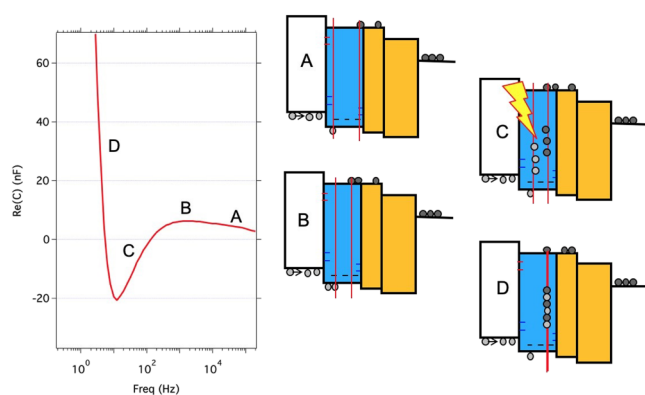
FIG. 4. Illustration for the interpretation of a negative capacitance in a QLED.

capacitance value equals its geometric capacitance. When the frequency decreases, shown in region B, charges become trapped and fewer are released from their trap states leading to charge accumulation and an increase in capacitance. When electrons and holes recombine, the total amount of charges within the active layer is reduced and therefore the capacitance decreases. A decrease in capacitance due to a population change, as shown in region C, is expected within a light out-coupling device. Up to this point, OLEDs and QLEDs behave very similarly as in both cases the capacitance can drop below 0. Whereas the organic devices show an only decreasing capacitance, their quantum dot counterparts typically show a negative and positive capacitance as illustrated in region D. In organic LEDs, a strong luminescent recombination along with little charge accumulation results in a decreasing capacitance. Trap states on the ligands surrounding the QD can store charges, preventing efficient transport to the recombination center and instead an internal capacitance builds up. When the threshold frequency is reached, this capacitance can no longer store charges and it releases charges under recombination current which appears as a negative capacitance. Therefore, a strong negative capacitance in QLEDs can be understood as an overinjection of charge carriers into the active layer, leading to an enhanced nonluminescent recombination. With the frequency further decreasing, charges become more stationary and fill the now vacant trap states and cannot be released. Consequently, the total capacitance of the device builds up, as shown in region D.

The formation of a recombination current and the increased charge carrier movement can limit the long term stability of the device.

Short and conductive amines show superior behavior as they enable a high device brightness and efficiency by transporting charges efficiently through the active layer. These ligands enable dense quantum dot packing, resulting in less chance of charge carriers being trapped. By further preventing an accumulation of charge carriers, the dielectric stress and the release of a recombination current are reduced. The capacitance drops only slightly but remains positive over the whole frequency range. However, efficiently transporting charge carriers through the device, while enhancing luminescent and reducing nonluminescent recombination, remains a challenge. We

propose that a strong negative capacitance is linked to an overinjection of charge carriers which leads to an increased charge carrier-accumulation time on the ligand. Assuming that only a defined number of electrons and holes can recombine at a given time, more charges are injected into the active layer than can recombine. This leads to an accumulation of charges and an increase in accumulation/storage time, as well as to nonluminescent recombination pathways becoming more dominant. Finally, the overinjection leads to the discharge of the internal capacitance under the formation of a recombination current, which looks like a NC in impedance spectroscopy.

In the OLED NC case, the applied bias is rather low and the luminescence efficiency is highest. The drop of capacitance is therefore related to the reduced accumulation of charge carriers and is dominated by a strong emissive recombination. The balance between accumulation and recombination shifts toward the latter, leading to a decrease of the overall capacitance. We believe that the overall time constant in this case should be reduced compared to the QLED case.

V. SUMMARY

Impedance spectroscopy and the study of capacitance have been used for the first time to determine the effects of ligand length on the recombination of charge carriers in QLEDs. When the conductivity of the active layer is lowered, charge carriers accumulate and create an internal capacitor within the QD layer. At high frequencies, the trap states play only a minor role. However, below a critical frequency, the capacitance discharges due to the formation of a recombination current and a negative capacitance is observed. If the frequency is further decreased, the capacitance returns to positive values again. A strong negative capacitance is linked to an overinjection of charge carriers, which leads to an enhanced nonluminescent recombination. A simple numerical model relates the impact of the accumulation and recombination of charge carriers to the total measured capacitance. QLEDs comprising QDs with short and conductive ligands exhibit superior performance, because charge carrier transport to QDs is facilitated.

SUPPLEMENTARY MATERIAL

See supplementary material for a description of the dielectric loss factor, spectroscopic characterisation of the QDs after ligand exchange, and voltage-current-luminescence data of the QLEDs.

ACKNOWLEDGMENTS

REFERENCES

[1]V. C. Bender, T. B. Marchesan, and J. M. Alonso, IEEE Ind. Electron. Mag. **9**, 6 (2015).
[2]T. Tsujimura, *OLED Display Fundamentals and Applications* (John Wiley & Sons, 2017).
[3]L. Ding, S.-C. Dong, Z.-Q. Jiang, H. Chen, and L.-S. Liao, Adv. Funct. Mater. **25**, 645 (2015).
[4]S. Zhang, L. Yao, Q. Peng, W. Li, Y. Pan, R. Xiao, Y. Gao, C. Gu, Z. Wang, P. Lu *et al.* Adv. Funct. Mater. **25**, 1755 (2015).
[5]B.-Q. Liu, L. Wang, D.-Y. Gao, J.-H. Zou, H.-L. Ning, J.-B. Peng, and Y. Cao, Light Sci. Appl. **5**, e16137 (2016).

[6] B. Liu, H. Nie, X. Zhou, S. Hu, D. Luo, D. Gao, J. Zou, M. Xu, L. Wang, Z. Zhao et al. Adv. Funct. Mater. **26**, 776 (2016).

[7] D. J. Gaspar and E. Polikarpov, *OLED Fundamentals: Materials, Devices, and Processing of Organic Light-Emitting Diodes* (CRC Press, 2015).

[8] P. O. Anikeeva, J. E. Halpert, M. G. Bawendi, and V. Bulovic, Nano Lett. **9**, 2532 (2009).

[9] Y. Shirasaki, G. J. Supran, M. G. Bawendi, and V. Bulović, Nat. Photonics **7**, 13 (2013).

[10] H. Shen, W. Cao, N. T. Shewmon, C. Yang, L. S. Li, and J. Xue, Nano Lett. **15**, 1211 (2015).

[11] J. Kwak, J. Lim, M. Park, S. Lee, K. Char, and C. Lee, Nano Lett. **15**, 3793 (2015). pMID: 25961530,

[12] K.-H. Lee, C.-Y. Han, H.-D. Kang, H. Ko, C. Lee, J. Lee, N. Myoung, S.-Y. Yim, and H. Yang, ACS Nano **9**, 10941 (2015).

[13] L. Sun, J. J. Choi, D. Stachnik, A. C. Bartnik, B.-R. Hyun, G. G. Malliaras, T. Hanrath, and F. W. Wise, Nat. Nanotechnol. **7**, 369 (2012).

[14] V. Colvin, M. Schlamp, and A. A. Nature, Nature **370**, 354–357 (1994).

[15] J. Li, Z. Liang, Q. Su, H. Jin, K. Wang, G. Xu, and X. Xu, ACS Appl. Mater. Interfaces **10**, 3865–3873 (2018).

[16] K.-H. Lee, J.-H. Lee, W.-S. Song, H. Ko, C. Lee, J.-H. Lee, and H. Yang, ACS Nano **7**, 7295 (2013).

[17] S. Nowy, W. Ren, J. Wagner, J. A. Weber, and W. Brütting, in *Organic Light Emitting Materials and Devices XIII* (International Society for Optics and Photonics, 2009), Vol. 7415, p. 74150G.

[18] T. Okachi, T. Nagase, T. Kobayashi, and H. Naito, Thin Solid Films **517**, 1331 (2008).

[19] T. Okachi, T. Nagase, T. Kobayashi, and H. Naito, Jpn. J. Appl. Phys. **47**, 8965 (2008).

[20] P. Chulkin, O. Vybornyi, M. Lapkowski, P. Skabara, and P. Data, J. Mater. Chem. C **6**, 1008 (2018).

[21] S. Nowy, W. Ren, A. Elschner, W. Lövenich, and W. Brütting, J. Appl. Phys. **107**, 054501 (2010).

[22] M. Ershov, H. Liu, L. Li, M. Buchanan, Z. Wasilewski, and A. K. Jonscher, IEEE Trans. Electron Devices **45**, 2196 (1998).

[23] A. Perera, W. Shen, M. Ershov, H. Liu, M. Buchanan, and W. Schaff, Appl. Phys. Lett. **74**, 3167 (1999).

[24] X. Wu, E. Yang, and H. Evans, J. Appl. Phys. **68**, 2845 (1990).

[25] G. Parravicini, A. Stella, M. Ungureanu, and R. Kofman, Appl. Phys. Lett. **85**, 302 (2004).

[26] J. Bisquert, G. Garcia-Belmonte, Á Pitarch, and H. J. Bolink, Chem. Phys. Lett. **422**, 184 (2006).

[27] E. Ehrenfreund, C. Lungenschmied, G. Dennler, H. Neugebauer, and N. Sariciftci, Appl. Phys. Lett. **91**, 012112 (2007).

[28] L. Pingree, B. Scott, M. Russell, T. Marks, and M. Hersam, Appl. Phys. Lett. **86**, 073509 (2005).

[29] M. Beale and P. Mackay, Philos. Mag. B **65**, 47 (1992).

[30] C. Zhu, L. Feng, C. Wang, H. Cong, G. Zhang, Z. Yang, and Z. Chen, Solid State Electron. **53**, 324 (2009).

[31] Ş. Çavdar, H. Koralay, N. Tuğluoğlu, and A. Günen, Superconductor Sci. Technol. **18**, 1204 (2005).

[32] M. Matsumura and Y. Hirose, Jpn. J. Appl. Phys. **39**, L123 (2000).

[33] K. Butcher, T. Tansley, and D. Alexiev, Solid State Electron. **39**, 333 (1996).

[34] C. Champness and W. Clark, Appl. Phys. Lett. **56**, 1104 (1990).

[35] T. Phillips and N. Gordon, J. Electron. Mater. **25**, 1151 (1996).

[36] V. González-Pedro, X. Xu, I. Mora-Sero, and J. Bisquert, ACS Nano **4**, 5783 (2010).

[37] I. Mora-Sero, S. Gimenez, F. Fabregat-Santiago, R. Gomez, Q. Shen, T. Toyoda, and J. Bisquert, Acc. Chem. Res. **42**, 1848 (2009).

[38] J. Wang, I. Mora-Seró, Z. Pan, K. Zhao, H. Zhang, Y. Feng, G. Yang, X. Zhong, and J. Bisquert, J. Am. Chem. Soc. **135**, 15913 (2013).

[39] A. Uddin and C. Teo, Appl. Phys. A **105**, 39 (2011).

[40] W. K. Bae, M. K. Nam, K. Char, and S. Lee, Chem. Mater. **20**, 5307 (2008).

[41] G. Paasch and S. Scheinert, Synth. Met. **122**, 145 (2001).

[42] V. Shrotriya and Y. Yang, J. Appl. Phys. **97**, 054504 (2005).

[43] S. Berleb, W. Brütting, and G. Paasch, Org. Electron. **1**, 41 (2000).

[44] H. Gommans, M. Kemerink, and R. Janssen, Phys. Rev. B **72**, 235204 (2005).

[45] F. Castro, P. Bueno, C. Graeff, F. Nüesch, L. Zuppiroli, L. Santos, and R. Faria, Appl. Phys. Lett. **87**, 013505 (2005).

Supplementay Material: Negative Capacitance as a Diagnostic Tool For Recombination in Purple Quantum Dot LEDs

I. REAL AND IMAGINARY PART OF CAPACITANCE

Capacitance C is defined as the ratio of change of charge ∂Q to the corresponding change in the applied electric potential ∂V and for a simple plate device, this is given by:

$$C = \frac{\partial Q}{\partial V} = \varepsilon_0 \hat{\varepsilon}_r \frac{A}{d} \tag{S1}$$

where ε_0 is the vacuum permittivity and ε_r is the relative permittivity of the material under investigation, d is the thickness of the layer and A is the area of the device. The time dependent dielectric response of the material, ε_r, to an external field is generally complex.

$$\hat{\varepsilon}_r = Re(\varepsilon_r) + jIm(\varepsilon_r) \tag{S2}$$

Here $Re(\varepsilon_r)$ represents the real part of the dielectric function of the material and $Im(\varepsilon_r)$ represents its imaginary counterpart, while j is the square root of -1. Therefore, capacitance C has a real part $Re(C)$ and an imaginary part $Im(C)$. The dielectric loss $tan(\delta)$ is defined as the quotient of the imaginary part of the relative permittivity over its real counterpart.

$$tan(\delta) = \frac{Im(\varepsilon_r)}{Re(\varepsilon_r)} \tag{S3}$$

This ratio can be understood as the quality factor of the capacitor since it relates the losses over the ability to store charge carriers. Through $\sigma_{ac} = 2\pi f \varepsilon_0 Re(\varepsilon_r) tan(\delta)$ the loss factor is directly proportional to the frequency (f) dependent ac-conductivity of the cavity.

In addition to capacitance, impedance spectroscopy measures the electrical impedance $\hat{Z} = Re(Z) + jIm(Z)$ of a device, with $Re(Z)$ being the real part of the impedance and $Im(Z)$ its imaginary counterpart. The electrical impedance is linked to the real part of the capacitance through equation S4

$$Re(C) = \frac{1}{2\pi f} \frac{-Im(Z)}{Re^2(Z) + Im^2(Z)} \tag{S4}$$

With this equation it becomes clear that a positive capacitance requires a negative value of $Im(Z)$ while a negative capacitance implies $Im(Z) > 0$.

II. OPTICAL AND ELECTRICAL PERFORMANCE OF QLEDS

Figure S1 shows the absorbance and fluorescence spectra for the QDs after the ligand exchange. The excitation wavelength for the fluorescence spectra was 370nm and the emission spectrum started at 390nm. Interestingly, the ligand length has no impact on the absorbance or photoluminescence spectrum of the QDs. The main peak in the EL spectrum can be attributed to QD emission, however, a secondary smaller peak at a slightly larger wavelength is attributed to trap emission from the charge transport layer. In a film a short ligand decreases the packing distance between QDs and decreases the turn-on voltage as shown in table I. Typically QLEDs with a very short ligand length have a rather short device lifetime.

Table I and figure S2 show a summary of V-I-L performance of the QLEDs with various ligands. V_{th} is the threshold voltage indicating the injection of holes into the device and V_{on} is the turn-on voltage ($V > 1cd/m^2$), with before efficiencies reported at V_{on}. Figure S3 shows the luminescence efficiency of a butylamine capped QLED.

With electrically insulating amines, both voltages shift to higher values with increasing ligand lengths. A longer amine chain length leads to lower electrical conductivity and a reduced QD packing density. Charge transport from the electrodes to the QDs is therefore reduced. Consequently, both the device efficiency and the brightness decrease. Despite a change in ligand length and conductivity, V_{th} and V_{on} are similar for both conductive amines. With its $\pi - \pi$ stacking, triphenylamine is the most conductive amine in this study and shows the highest efficiency. Overall, a short and conductive amine leads to an increased brightness.
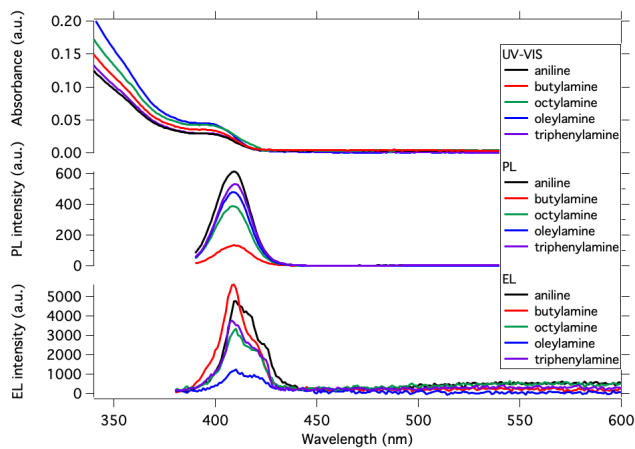
FIG. S1: Absorbance, fluorescence and electroluminescence spectra of the QDs after ligand exchange.
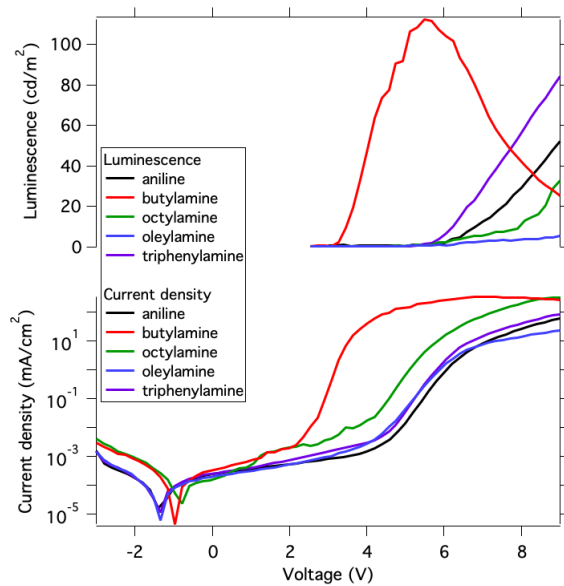

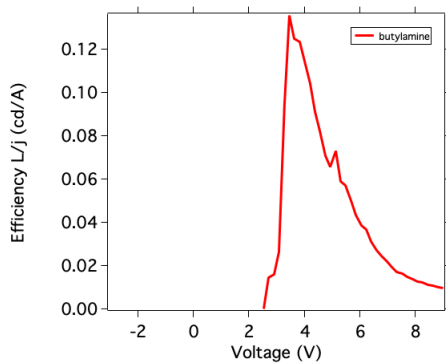FIG. S2: Voltage-current density-luminescence diagram for the QLEDs with the ligands under test.

FIG. S3: Typical luminescence efficiency of a butylamine capped QLED.

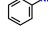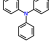| amine			V_{th} (V)	$V_{on}(V)$	efficiency (cd/A)	max. brightness (cd)
butylamine		insulating	2.8	2.8	0.14	112
octylamine			3.5	5.1	0.09	31
oleylamine			5.0	7.1	<0.03	5
aniline		conductive	4.0	5.9	0.15	52
triphenylamine			5.0	6.2	0.25	83

TABLE I: Overview of the I-V performance of the QLEDs with various ligands.